

Design, Synthesis, and Biological Evaluation of Novel Pyrazine Substituted Benzamides as Allosteric Activators of Human Glucokinase

Prateek Sharma^{1,2} , Anju Goyal¹ , Ajmer Singh Grewal^{3,*} 

¹ Chitkara College of Pharmacy, Chitkara University, Punjab, India

² Government Pharmacy College, Nagrota Bagwan, Kangra, Himachal Pradesh, India

³ Guru Gobind Singh College of Pharmacy, Yamunanagar, Haryana, India

* Correspondence: ajmergrewal2007@gmail.com;

Received: 29.10.2023; Accepted: 7.07.2024; Published: 6.09.2025

Abstract: Glucokinase (GK) serves as the primary enzyme for regulating human blood glucose levels within a narrow physiological range. GK activators represent a promising class of therapeutic agents showing promising effects in the treatment of diabetes. The aim of this study was to design a novel class of benzamide derivatives with pyrazine substitutions, intending them to function as potential activators of GK and subsequently assess their efficacy in managing diabetes. Starting with benzoic acid, numerous pyrazine-substituted benzamides were synthesized and subsequently subjected to *in vitro* experiments to assess their ability to activate GK. Docking studies were employed to determine the binding interactions for the most suitable conformations in the allosteric region of GK. The antihyperglycemic efficacy of the selected compounds was assessed using the oral glucose tolerance test (OGTT) in normal rats, guided by the results of both *in vitro* enzyme assays and *in silico* investigations. After identifying one of the most potent compounds from the antihyperglycemic assay, it underwent additional evaluation for its antidiabetic effects in an OGTT assay using induced diabetic rats. *In vitro*, activation of GK revealed that compounds 1, 8, and 9 exhibited the highest activation, with activation fold values ranging between 1.90 and 2.10. Subsequent OGTT (normal rats) demonstrated promising antihyperglycemic activity for compounds 1 and 8. Confirming consistency with both docking studies and *in vitro* results, the *in vivo* antidiabetic assay underscored the potential therapeutic efficacy of the tested compound. The newly synthesized pyrazine-substituted benzamide derivatives serve as promising candidates for the development of allosteric activators of human GK. These compounds exhibit safety, efficacy, and oral bioavailability attributes, making them potential therapeutic substances for type 2 diabetes management.

Keywords: diabetes; antidiabetic study; glucokinase; allosteric human gk activators; benzamide derivatives.

© 2025 by the authors. This article is an open-access article distributed under the terms and conditions of the Creative Commons Attribution (CC BY) license (<https://creativecommons.org/licenses/by/4.0/>), which permits unrestricted use, distribution, and reproduction in any medium, provided the original work is properly cited. The authors retain copyright of their work, and no permission is required from the authors or the publisher to reuse or distribute this article, as long as proper attribution is given to the original source.

1. Introduction

The International Diabetes Federation (IDF) has recently released updated statistics indicating a significant global increase in the prevalence of diabetes. According to the latest IDF Diabetes Atlas, the global prevalence of diabetes has risen by approximately 16% since 2019, with a current estimate of 537 million people affected globally. This growth corresponds to an additional 74 million individuals living with diabetes. The current worldwide incidence

of diabetes is 10.5%, and approximately half of those with diabetes are unaware of their condition. The IDF predicts that by 2045, there will be 783 million individuals with diabetes worldwide, equating to one in eight adults, a 46% increase surpassing the expected population growth of 20% during the same period. Excluding the risks of death related to COVID-19, it is anticipated that almost 6.7 million individuals will die from diabetes or its complications in 2021, accounting for more than one in ten (12.2%) of all worldwide fatalities [1]. In individuals with diabetes, increased blood glucose levels, known as hyperglycemia, result from insufficient insulin or insulin resistance. Despite the availability of various oral drugs, both single-drug treatment and combination therapies have shown insufficient efficacy in maintaining optimal blood glucose control, mainly due to the potential for hypoglycemia and other toxic consequences. Consequently, there has been an accelerated focus on research to identify targets and develop novel chemical entities to enhance therapeutic approaches [2-5]. Type 1 diabetes, marked by a gradual decline in insulin secretion by β -cells in the pancreas, represents an estimated 5-10% of all diabetes cases. In contrast, type 2 diabetes mellitus (T2DM), accounting for around 90-95% of all diabetes cases, represents a chronic ailment of energy metabolism involving impaired glucose breakdown and diminished insulin action. Despite the array of available diabetes treatments, no single medication has proven effective in achieving sustained regulation of glycemic content in most people diagnosed with diabetes. Consequently, physicians increasingly advocate for early combination therapy with antidiabetic agents [6-9]. Overdosing on antidiabetic drugs can lead to severe hypoglycemia with associated toxic effects, necessitating immediate medical care. The research community is presently involved in the development of novel, safe, and therapeutically unique antidiabetic medicines for use as monotherapy with improved efficacy. Recent research incorporating emergent clinical data emphasizes the potential of small-molecule glucokinase (GK) activators in addressing this need [10]. GK, an enzyme situated within cells, catalyzes the conversion of glucose into glucose-6-phosphate (G-6-P) through a phosphorylation reaction. Additionally, GK functions as a molecular sensor in pancreatic β -cells, establishing a connection between blood glucose levels and insulin production via complex signaling pathways, thereby regulating glucose-stimulated insulin secretion (GSIR). GK plays a crucial role in controlling glucose metabolism, emerging as a potential therapeutic target for type 2 diabetes. Primarily located in pancreatic β -cells and liver hepatocytes, GK regulates insulin release in response to glucose in the pancreas and governs carbohydrate metabolism in hepatocytes. GK activators, a new class of potential drug candidates, demonstrate hypoglycemic activity by modulating the GK enzyme [10-13]. Various molecules belonging to different chemical classes have been investigated in recent years for their potential as GK activators. These include benzamides [14-30], acetamides [31,32], carboxamides [33,36], acrylamides [37], benzimidazoles [38,39], quinazolines [40], thiazoles [41,42], pyrimidines [43,44], and urea derivatives [45-53]. While researchers explore multiple chemical moieties as GK activators, the predominant focus has been on benzamide derivatives due to their distinctive orientations and binding behaviors within the allosteric site. A wide range of molecules with potential as GK activators can be generated by incorporating diverse functional groups onto the phenyl ring and the amide -NH moiety. Our group recently identified novel benzamide compounds with potential GK activation properties [26-30]. Aligning with numerous research findings and recognizing the pivotal significance of GK activators in managing T2DM, novel allosteric activators of the human GK were designed and synthesized using the benzamide scaffold. The benzamide core was selectively substituted to establish robust binding interactions with residues in the allosteric region of GK. Furthermore,

the proposed derivatives were designed for oral bioavailability by incorporating groups such as sulphonamides into the benzamide scaffold.

2. Materials and Methods

2.1. Materials.

The study's chemicals, materials, solvents, and proteins were procured from reputable sources, including SRL, Spectrochem, Sigma-Aldrich, Merck, S.D. Fine-Chem, LOBA, Fisher Scientific, etc., and utilized in their original state without further modification. Melting points were determined using a Veego VMP-D melting point apparatus (open capillary tubes). The progress of the reaction was monitored through thin-layer chromatography (TLC) on silica gel-G plates. The confirmation of compound purity was established by the presence of a single spot on the TLC plate. Infrared (IR) bands were recorded using a Bruker make alpha 2 opus program. The ^{13}C NMR spectra were obtained on a 100 MHz NMR spectrophotometer, while the ^1H NMR spectra were collected on a Bruker Avance II 300 MHz NMR spectrophotometer using dimethyl sulfoxide (DMSO)- d_6 as a solvent. The results are expressed in parts per million (δ , ppm), referenced to tetramethylsilane (used as an internal standard), and presented as downfield values.

2.2. *In silico* prediction of pharmacokinetics.

The proposed compounds' drug-likeness characteristics were assessed using the SwissADME tool (<http://www.swissadme.ch/>) [54]. The drug-likeness of the compounds was evaluated based on Lipinski's rule of five [55].

2.3. Synthesis.

In a flat-bottom flask equipped with a magnetic stirrer, 0.01 moles of dry benzoic acid were placed. To maintain a steady temperature between 10-15°C, the flask was immersed in a cold-water bath. Carefully adding 8.0 mL of chlorosulphonic acid, ensuring no leakage, initiated an exothermic reaction. Once the acid completely dissolved and the exothermic reaction ceased, the flask's contents were heated in a water bath within the temperature range of 70-80°C for 2 hours to ensure completion of the reaction. The vessel was then cooled. To disintegrate any clumps, the flask contents were added to 150 g of crushed ice while stirring. The resulting precipitates of 3-(chlorosulfonyl)benzoic acid were filtered using a vacuum filter and rinsed with cold water before being left to air dry. The previously obtained product (0.01 mol) underwent reflux with commercially available amines (0.01 mol) in acetone. The reaction continued until completion, as determined by TLC on silica gel G. After cooling, the resulting sulphonamides were allowed to air dry. Subsequently, the different sulphonamides (0.01 mol) were refluxed with thionyl chloride (0.01 mol) for 3 hours in acetone. Excess thionyl chloride was removed through distillation to obtain appropriate benzoyl chlorides. These benzoyl chlorides (0.01 mol) were then refluxed with 2-amino-pyrazine (0.015 mol) in acetone. After evaporating the acetone, the resulting products (pyrazine-substituted benzamides) were purified via recrystallization using ethyl alcohol [56-57].

2.3.1. 3-[(2-Bromophenyl)sulfamoyl]-N-(pyrazin-2-yl)benzamide (1)

FTIR (ν cm^{-1}): 3366.65, 3224.36, 3040.91, 1694.53, 1639.75, 1591.34, 1514.25, 1341.60, 1297.09, 1179.69, 696.25, 659.30; $^1\text{H-NMR}$ (δ ppm, 300 MHz, DMSO- d_6): 8.75 (s, 1H, NH, Amide), 8.30-8.40 (m, 4H, 4CH, $\text{C}_6\text{H}_4\text{CO}$), 7.26 (s, 1H, NH, $\text{SO}_2\text{-NH}$), 6.40-8.30 (m, 3H, 3CH, Pyrazin-2-yl), 7.11-7.62 (m, 4H, 4CH, 2- BrC_6H_4); $^{13}\text{C-NMR}$ (δ ppm, 100 MHz, DMSO- d_6): 163.8 (C=O, Amide), 134.0 (C, C_1 , C_6H_4), 122.3 (CH, C_2 , C_6H_4), 139.5 (C, C_3 , C_6H_4), 131.0 (CH, C_4 , C_6H_4), 129.0 (CH, C_5 , C_6H_4), 129.8 (CH, C_6 , C_6H_4), 148.0 (C, C_2 , Pyrazin-2-yl), 136.1 (CH, C_3 , Pyrazin-2-yl), 138.4 (CH, C_5 , Pyrazin-2-yl), 138.5 (CH, C_6 , Pyrazin-2-yl), 134.5 (C, C_1 , 2- BrC_6H_4), 116.7 (C, C_2 , 2- BrC_6H_4), 131.4 (CH, C_3 , 2- BrC_6H_4), 126.5 (CH, C_4 , 2- BrC_6H_4), 126.2 (CH, C_5 , 2- BrC_6H_4), 121.8 (CH, C_6 , 2- BrC_6H_4); HRMS (ESI TOF) m/z for $\text{C}_{17}\text{H}_{13}\text{BrN}_4\text{O}_3\text{S}$ $[\text{M}+\text{H}]^+$: Calculated: 433.281, Found: 432.5.

2.3.2. 3-(Ethylsulfamoyl)-N-(pyrazin-2-yl)benzamide (2).

FTIR (ν cm^{-1}): 3390.19, 3361.88, 2923.92, 2856.58, 1694.10, 1516.77, 1461.45, 1352.72, 1310.67, 1168.82, 1023.78, 838.53; $^1\text{H-NMR}$ (δ ppm, 300 MHz, DMSO- d_6): 8.75 (s, 1H, NH, Amide), 8.32-8.42 (m, 4H, 4CH, $\text{C}_6\text{H}_4\text{CO}$), 7.26 (t, 1H, NH, $\text{SO}_2\text{-NH}$), 6.55-8.35 (m, 4H, 4 CH, Pyrazin-2-yl), 2.50 (m, 4H, CH, CH_2), 1.10 (t, 3H, CH, CH_3).

2.3.3. 3-(Butylsulfamoyl)-N-(pyrazin-2-yl)benzamide (3).

FTIR (ν cm^{-1}): 3347.97, 3167.36, 3081.51, 2858.91, 1691.68, 1630.03, 1602.03, 1506.07, 1400.97, 1139.10, 784.96; $^1\text{H-NMR}$ (δ ppm, 300 MHz, DMSO- d_6): 8.75 (s, 1H, NH, Amide, Benzamide), 8.30-8.40 (m, 4H, 4CH, $\text{C}_6\text{H}_4\text{CO}$), 7.32 (t, 1H, NH, $\text{SO}_2\text{-NH}$, Sulphonamide), 6.50-8.35 (m, 3H, 3CH, Pyrazin-2-yl), 2.65 (m, 3H, CH_2 , Butyl), 2.30 (m, 4H, CH_2 , Butyl), 2.28 (m, 5H, CH_2 , Butyl), 1.12 (t, 2H, CH_3 , Butyl).

2.3.4. 3-(Hydroxysulfamoyl)-N-(pyrazin-2-yl)benzamide (4).

FTIR (ν cm^{-1}): 3543.63, 3350.71, 3167.24, 3080.24, 1693.51, 1514.39, 832.55; $^1\text{H-NMR}$ (δ ppm, 300 MHz, DMSO- d_6): 8.90 (s, 1H, NH, Amide), 8.32-8.46 (m, 4H, 4CH, $\text{C}_6\text{H}_4\text{CO}$), 7.20 (d, 1H, NH, $\text{SO}_2\text{-NH}$), 6.55-8.30 (m, 3H, CH, Pyrazin-2-yl), 2.30 (d, 1H, OH, NH-OH).

2.3.5. 3-(Hydrazinesulfonyl)-N-(pyrazin-2-yl)benzamide (5).

FTIR (ν cm^{-1}): 3534.50, 3391.36, 2923.24, 2856.11, 1741.97, 1515.74, 1459.05, 1386.35, 1250.89, 1167.71, 832.99; $^1\text{H-NMR}$ (δ ppm, 300 MHz, DMSO- d_6): 8.75 (s, 1H, NH, Amide), 8.30-8.40 (m, 4H, 4CH, $\text{C}_6\text{H}_4\text{CO}$), 7.16 (s, 1H, NH, $\text{SO}_2\text{-NH}$), 6.50-8.35 (m, 3H, 3CH, Pyrazin-2-yl), 2.30 (d, 1H, NH, NH- NH_2 , Hydrazine).

2.3.6. 3-(Phenylsulfamoyl)-N-(pyrazin-2-yl)benzamide (6).

FTIR (ν cm^{-1}): 3397.70, 3281.12, 3114.53, 1695.42, 1515.60, 1481.31, 1461.81, 1160.99, 1093.51, 790.30; $^1\text{H-NMR}$ (δ ppm, 300 MHz, DMSO- d_6): 8.72 (s, 1H, NH, Amide, Benzamide), 8.30-8.40 (m, 4H, 4CH, $\text{C}_6\text{H}_4\text{CO}$), 7.15 (s, 1H, NH, $\text{SO}_2\text{-NH}$), 6.50-8.32 (m, 3H, 3CH, Pyrazin-2-yl), 7.05-7.60 (m, 5H, 5CH, C_6H_5).

2.3.7. N-(Pyrazin-2-yl)-3-sulfamoylbenzamide (7).

FTIR (ν cm^{-1}): 3432.83, 2998.06, 2914.21, 1658.37, 1436.17, 1311.90, 1016.45, 699.27; $^1\text{H-NMR}$ (δ ppm, 300 MHz, DMSO- d_6): 8.75 (s, 1H, NH, Amide), 8.30-8.40 (m, 4H, 4CH, $\text{C}_6\text{H}_4\text{CO}$), 7.09 (s, 1H, NH, $\text{SO}_2\text{-NH}_2$), 6.50-8.35 (m, 3H, 3CH, Pyrazin-2-yl).

2.3.8. 3-[(2-Chlorophenyl)sulfamoyl]-N-(pyrazin-2-yl)benzamide (8).

FTIR (ν cm^{-1}): 3327.89, 2924.63, 1658.91, 1596.37, 1532.37, 1467.07, 1383.26, 1215.44, 1112.54, 744.88, 693.36; $^1\text{H-NMR}$ (δ ppm, 300 MHz, DMSO- d_6): 8.75 (s, 1H, NH, Amide), 8.30-8.40 (m, 4H, 4CH, $\text{C}_6\text{H}_4\text{CO}$), 7.32 (s, 1H, NH, $\text{SO}_2\text{-NH}$), 6.50-8.32 (m, 3H, 3CH, Pyrazin-2-yl), 7.10-7.58 (m, 4H, 4CH, 2- ClC_6H_4); $^{13}\text{C-NMR}$ (δ ppm, 100 MHz, DMSO- d_6): 163.8 (C=O, Amide), 133.8 (C, C_1 , C_6H_4), 130.7 (CH, C_2 , C_6H_4), 130.0 (C, C_3 , C_6H_4), 131.0 (CH, C_4 , C_6H_4), 140.0 (CH, C_5 , C_6H_4), 120.0 (CH, C_6 , C_6H_4), 150.0 (C, C_2 , Pyrazin-2-yl), 136.5 (CH, C_3 , Pyrazin-2-yl), 136.2 (CH, C_5 , Pyrazin-2-yl), 139.2 (CH, C_6 , Pyrazin-2-yl), 128.0 (C, C_1 , 2- ClC_6H_4), 125.5 (C, C_2 , 2- ClC_6H_4), 131.5 (CH, C_3 , 2- ClC_6H_4), 124.8 (CH, C_4 , 2- ClC_6H_4), 127.5 (CH, C_5 , 2- ClC_6H_4), 121.5 (CH, C_6 , 2- ClC_6H_4); HRMS (ESI TOF) m/z for $\text{C}_{17}\text{H}_{13}\text{ClN}_4\text{O}_3\text{S}$ $[\text{M}+\text{H}]^+$: Calculated: 388.830, Found: 388.5.

2.3.9. 3-(Propylsulfamoyl)-N-(pyrazin-2-yl)benzamide (9).

FTIR (ν cm^{-1}): 3430.49, 2997.85, 2914.34, 1658.64, 1436.11, 1311.90, 1016.40, 699.34; $^1\text{H-NMR}$ (δ ppm, 300 MHz, DMSO- d_6): 8.90 (s, 1H, NH, Amide), 8.30-8.42 (m, 4H, 4CH, $\text{C}_6\text{H}_4\text{CO}$), 7.26 (t, 1H, NH, $\text{SO}_2\text{-NH}$), 6.50-8.34 (m, 3H, 3CH, Pyrazin-2-yl), 2.70 (m, 3H, CH_2 , Propyl), 2.29 (m, 5H, CH_2 , Propyl), 1.10 (t, 2H, CH_3 , Propyl); $^{13}\text{C-NMR}$ (δ ppm, 100 MHz, DMSO- d_6): 163.7 (C=O, Amide), 134.0 (C, C_1 , C_6H_4), 120.5 (CH, C_2 , C_6H_4), 140.0 (C, C_3 , C_6H_4), 131.5 (CH, C_4 , C_6H_4), 130.0 (CH, C_5 , C_6H_4), 131.5 (CH, C_6 , C_6H_4), 150.0 (C, C_2 , Pyrazin-2-yl), 135.8 (CH, C_3 , Pyrazin-2-yl), 137.5 (CH, C_5 , Pyrazin-2-yl), 139.8 (CH, C_6 , Pyrazin-2-yl), 43.0 (CH_2 , Propyl), 21.2 (CH_2 , Propyl), 10.5 (CH_3 , Propyl); HRMS (ESI TOF) m/z for $\text{C}_{14}\text{H}_{16}\text{N}_4\text{O}_3\text{S}$ $[\text{M}+\text{H}]^+$: Calculated: 320.372, Found: 319.8.

2.3.10. 3-[(2-Nitrophenyl)sulfamoyl]-N-(pyrazin-2-yl)benzamide (10).

FTIR (ν cm^{-1}): 3579.45, 3234.43, 2923.17, 1698.47, 1515.56, 1460.43, 1162.87, 1028.08, 822.51; $^1\text{H-NMR}$ (δ ppm, 300 MHz, DMSO- d_6): 8.73 (s, 1H, NH, Amide), 8.30-8.42 (m, 4H, 4CH, $\text{C}_6\text{H}_4\text{CO}$), 7.18 (s, 1H, NH, $\text{SO}_2\text{-NH}$), 6.50-8.32 (m, 3H, 3CH, Pyrazin-2-yl), 7.10-7.59 (m, 4H, 4CH, 2- $\text{NO}_2\text{C}_6\text{H}_4$).

2.3.11. 3-[(4-Nitrophenyl)sulfamoyl]-N-(pyrazin-2-yl)benzamide (11).

FTIR (ν cm^{-1}): 3545.23, 3398.69, 2923.34, 1679.92, 1641.98, 1564.34, 1548.43, 1512.08, 1452.90, 704.51; $^1\text{H-NMR}$ (δ ppm, 300 MHz, DMSO- d_6): 8.72 (s, 1H, NH, Amide), 8.30-8.42 (m, 4H, 4CH, $\text{C}_6\text{H}_4\text{CO}$), 7.26 (s, 1H, NH, $\text{SO}_2\text{-NH}$), 6.50-8.32 (m, 3H, 3CH, Pyrazin-2-yl), 7.10-7.59 (m, 4H, 4CH, 4- $\text{NO}_2\text{C}_6\text{H}_4$).

2.3.12. 3-(2-Phenylhydrazinesulfonyl)-N-(pyrazin-2-yl)benzamide (12).

FTIR (ν cm^{-1}): 3392.44, 3256.19, 2923.11, 2855.98, 1695.33, 1516.45, 1251.02, 812.38; $^1\text{H-NMR}$ (δ ppm, 300 MHz, DMSO- d_6): 8.75 (s, 1H, NH, Amide, Benzamide), 8.30-

8.40 (m, 4H, 4CH, C₆H₄CO), 7.09 (s, 1H, NH, SO₂-NH), 6.49-8.31 (m, 3H, 3CH, Pyrazin-2-yl), 7.12-7.64 (m, 5H, 5CH, C₆H₅).

2.3.13. 3-(Benzylsulfamoyl)-N-(pyrazin-2-yl)benzamide (13).

FTIR (ν cm⁻¹): 3430.80, 2998.25, 2914.77, 1658.45, 1436.19, 1406.87, 1311.99, 1016.31, 699.44; ¹H-NMR (δ ppm, 300 MHz, DMSO-d₆): 8.75 (s, 1H, NH, Amide), 8.30-8.40 (m, 4H, 4CH, C₆H₄CO), 7.23 (t, 1H, NH, SO₂-NH), 6.50-8.32 (m, 3H, 3CH, Pyrazin-2-yl), 7.10-7.59 (m, 5H, 5CH, C₆H₅), 3.30 (d, 1H, CH, CH₂ of Benzyl).

2.4. *In vitro* GK assay.

The GK activity of the synthesized compounds was spectrometrically assessed through a coupled reaction with glucose-6-phosphate dehydrogenase (G-6-PDH). Proteins and reagents for the assay were obtained from Sigma-Aldrich and SRL. All compounds were prepared in DMSO, and the assay was conducted in a final volume of 2000 μ L, comprising 25 mM 2-(4-(2-hydroxyethyl)piperazin-1-yl)ethane sulfonic acid (pH 7.4), 10 mM glucose, 25 mM KCl, 1 mM MgCl₂, 1 mM dithiothreitol, 1 mM adenosine triphosphate, 1 mM nicotinamide adenine dinucleotide, 2.5 U/mL G-6-PDH, 0.5 μ g GK, and synthesized compounds (10 μ M). Upon initiating the reaction, the increase in absorbance at 340 nm was monitored over a 3-minute incubation period as a measure of GK enzyme activity. The synthesized compounds' fold activation of the enzyme was calculated by comparing it with the control (GK activation with only DMSO was considered 100%) [27-30].

2.5. *In vivo* evaluation.

Wistar rats (150-200 g) were procured from Lala Lajpat Rai University of Veterinary and Animal Sciences, Hisar. The rats were housed in a controlled environment, maintaining room temperature at 22 \pm 2 $^{\circ}$ C, humidity at 55 \pm 5%, and light-dark cycles of 12 hours each. A standard pellet diet and unrestricted access to water were provided to the animals before the initiation of any dietary interventions. All procedures conducted in this study adhered to the rules stipulated by the "Committee for the Purpose of Control and Supervision of Experiments on Animals", Government of India (Approval No. GGSCOP/IAEC/May2023/8). The research was carried out in compliance with the guidelines established by the "Institutional Animal Ethics Committee" (IAEC).

2.5.1. OGTT (oral glucose tolerance test) in normal rats (antihyperglycemic study).

Based on an *in vitro* GK assay, the effects of three pyrazine-substituted benzamides (1, 8, and 9) were evaluated using oral glucose tolerance tests in healthy rats. There were five different groups of rats, each consisting of six subjects. Prior to treatment, each animal underwent a minimum eight-hour fasting period overnight. Group I, the control group, received treatment with 0.5% CMC (p.o.). Group II was administered a metformin dosage of 30 mg/kg (p.o.). Compounds 1, 8, and 9 were given to Groups III-V at a dosage of 50 mg/kg (p.o.). All groups received an oral dose of glucose at 3 g/kg (body weight) 30 minutes after the initiation of drug administration. Blood samples were collected from the tail vein before the administration of compounds and at 0, 30-, 60-, 90-, and 120 minutes post-glucose administration. A glucose testing kit promptly assessed the blood glycemic content level [27-

30]. To determine the area under the curve (AUC) for glucose, blood glucose data collected over a period of 0 to 2 hours were analyzed.

2.5.2. OGTT assay in induced diabetic rats (antidiabetic study).

Compound 8's antidiabetic activity was evaluated in an OGTT assay using induced diabetic rats based on the outcomes of the antihyperglycemic study conducted on normal rats. The study included six distinct groups of rats, with each group comprising six individual rats. Before treatment, all animals had a fasting period of at least 8 hours and had unrestricted access to a regular diet and water. The rats were housed in polyurethane enclosures under controlled room temperature and relative humidity conditions, experiencing a regular 12-hour period of light followed by 12 hours of darkness. Hyperglycemia was induced in all fasted rats (except the normal control group) by injecting alloxan monohydrate at 150 mg per kg of body weight, dissolved in normal saline, and administered intraperitoneally (i.p.). After 72 hours, blood sugar levels were assessed using a glucometer, and only rats displaying hyperglycemia were selected for subsequent study. The control groups, both normal and diabetic, were given only the vehicle (0.5% CMC solution, p.o.). The standard group received metformin treatment at a dosage of 30 mg/kg body weight, delivered orally, while the test groups received compound 8 at varying doses (25, 50, and 100 mg/kg body weight, p.o.). Each animal received an oral dose of glucose at 3 g/kg (body weight) precisely 30 minutes after the administration of the drug. Blood samples were collected from the tail vein of the animals before drug administration, as well as after 0-, 2-, 4-, and 6-hours following glucose loading. Immediate measurement of serum glucose levels was performed using a glucometer and the glucose oxidase technique [58-59].

2.6. *In silico* docking study.

In silico docking analyses of the designed molecules were conducted using AutoDock Vina within the allosteric region of the GK [60], utilizing AutoDock Tools installed on Windows 11 [61]. Marvin Sketch was employed to generate the 2-D structures of the ligands, which were subsequently converted into three-dimensional structures using the Frog2 server [62]. The ligands were configured for docking using AutoDock Tools, and PDBQT files were generated using the ligands' MOL format. The co-crystallized GK data were obtained from the RCSB Protein Data Bank. After a thorough evaluation of multiple entries, the optimal ligand-bound complex (PDB entry: 3IMX) was chosen through a detailed examination of its 3-D structures (based on the low resolution of the ligand-protein complex and binding interactions of the ligand with the protein). The complexed activator and all water molecules and ions that were not interacting were removed from the PDB file using PyMOL (Schrodinger, LLC). Protein processing and the creation of the PDBQT file from the PDB file were performed using AutoDock Tools, with the addition of all polar hydrogen atoms. The macromolecule was docked, and grid settings were determined through the "Grid" function in AutoDock Tools. A configuration file named "conf.txt" was created, presenting extensive information on the search space's grid dimensions, protein and ligand characteristics, and geometric properties. To evaluate the reliability of the docking approach, the reference ligand was initially docked into the GK's active site, and the resulting binding pose was compared with that of the co-crystallized GK activator. Ligand molecules were docked using AutoDock Vina, and techniques were employed to determine the rankings of the docked ligands. After completing

the docking process, the specific ligand pose with the most favorable binding free energy (ΔG) was selected. A more in-depth analysis of hydrogen bonds, hydrophobic interactions, and other significant aspects of the docked poses was conducted using PyMOL and Discovery Studio (Dassault Systèmes, Biovia Corp) [63-67].

2.7. *In silico* toxicity evaluation.

The pyrazine-substituted benzamide derivatives underwent *in silico* evaluation to assess their potential toxicity. This evaluation was performed utilizing the pkCSM web-based application [68-69].

3. Results and Discussion

3.1. *In silico* drug-likeness.

The SwissADME online platform provides complimentary access to a reliable set of prediction models for various physicochemical attributes, pharmacokinetics, drug compatibility, and suitability for medicinal chemistry [54]. *In silico* ADME prediction was conducted due to laboratory studies' time and cost constraints. Ensuring the success of a potential lead chemical in clinical trials is a crucial step. An optimal drug is characterized by rapid absorption, uniform distribution across the body, efficient metabolism, and excretion without adverse side effects. The characteristics typically seen in "drug-like" molecules include a molecular weight not exceeding 500, a log P value of 5 or less (milog), and a maximum of 10 hydrogen bond acceptors, with generally no more than 5 hydrogen bond donors, as specified by Lipinski's rule of five (RO5) for drug-likeness. Conducting a more in-depth analysis of the compounds adhering to these criteria helps in selecting candidates for further development [55]. Every developed compound adhered to Lipinski's rule of five (RO5), as indicated in Table 1.

Table 1. Predicted physicochemical characteristics of the designed pyrazine-substituted benzamide derivatives.

Compound	M.W.	HBA	HBD	TPSA (Å ²)	Log P	Sol.	GI ab	BBB	PGP	Lipinski #
1	433.28	5	2	109.43	1.52	+	High	No	No	0
2	306.34	6	2	109.43	1.02	+++	High	No	No	0
3	334.39	6	2	109.43	1.46	++	High	No	No	0
4	294.29	7	3	129.66	0.6	+++	High	No	No	0
5	293.30	7	3	135.45	0.23	+++	High	No	No	0
6	354.38	5	2	109.43	1.53	++	High	No	No	0
7	278.29	6	2	123.42	0.40	+++	High	No	No	0
8	388.83	5	2	109.43	1.44	++	High	No	No	0
9	320.37	6	2	109.43	1.25	++	High	No	No	0
10	399.38	7	2	155.25	1.02	++	Low	No	No	0
11	399.38	7	2	155.25	0.86	++	Low	No	No	0
12	369.40	6	3	121.46	1.50	++	High	No	No	0
13	368.41	6	2	109.43	1.99	++	High	No	No	0

M.W.: Mol. weight; HBA: Number of H-bond acceptors; HBD: Number of H-bond donors; TPSA: Topological polar surface area; Log P: Partition coefficient, Log P_{ow} (iLOGP); Sol.: Solubility class; +++: Very soluble; ++: Soluble, +: Moderately soluble; GI ab: GI absorption; BBB: BBB penetration; PGP: PGP substrate; Lipinski #: No. of violations to Lipinski's rule of 5.

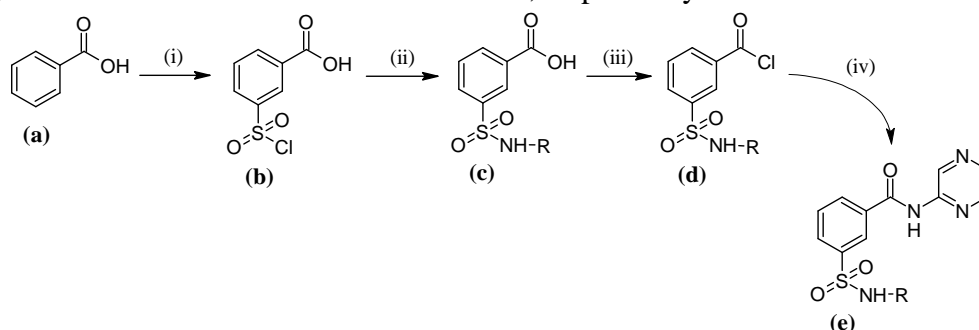
Since all these designed derivatives demonstrated promising characteristics for medication development, Table 1 shows that most compounds exhibited a notable degree of gastrointestinal (GI) absorption. Moreover, it was determined that all the proposed compounds are not P-glycoprotein (PGP) substrates. The impermeability of the blood-brain barrier (BBB)

suggests that these compounds are not likely to cross into the brain. Overexpression of P-glycoprotein (PGP) in the gastrointestinal tract can hinder the uptake of drugs into blood capillaries.

3.2. Chemistry.

The procedure for synthesizing the designed molecules is outlined in Scheme 1. In summary, 3-(chlorosulfonyl)benzoic acid (b), prepared by chloro sulfonation of benzoic acid (a), was refluxed with commercially available amines to obtain the proposed sulphonamides (c). The benzoyl chlorides (d), obtained via the refluxing of the aforementioned products with thionyl chloride, were then subjected to reflux with 2-amino-pyrazine to synthesize the intended pyrazine-substituted benzamides (e). The final products were produced with satisfactory yields (Table 2). The synthesized compounds underwent characterization using FTIR, ¹H-NMR, ¹³C-NMR, and mass spectroscopy.

The proton NMR spectral characterization of the prepared analogs revealed a singlet signal corresponding to one proton of the carboxamide (CONH) scaffold at around δ 9.0 ppm. This observation provides evidence for the formation of a benzamide bond in all the synthesized compounds. The occurrence of a singlet signal for one NH proton at about δ 7.20 ppm for the sulphonamide (SO₂NH) group indicates the formation of sulphonamide derivatives through the reaction between the corresponding amines and derivatives of sulphonyl chloride. The presence of a single signal (related to C₂), two doublet signals (related to C₄ and C₆), and a double doublet signal (related to C₅) within the δ 7.5-8.0 ppm range on the benzamide scaffold confirms the meta positioning of the benzamide and sulphonamide functional groups about each other. In the ¹H-NMR spectra, two doublet and one singlet signals corresponding to 3 protons (aromatic CH) were detected at about δ 6.5-8.0 ppm, affirming the synthesis of the intended derivatives through the reaction of benzoyl chloride with 2-amino-pyrazine. The ¹³C-NMR spectra signal around δ 165 ppm indicated the presence of a carbonyl (amide) bond, supporting the formation of the benzamide linkage in these derivatives. FTIR spectra of the prepared compounds displayed NH- vibrations (str.) (indicating the presence of an amide) above 3500 cm⁻¹. Additionally, CH- stretching (aromatic) vibrations were observed above 3000 cm⁻¹. The spectra also revealed SO₂ stretching vibrations, both asymmetric and symmetric, in the range of 1399-1301 cm⁻¹ and 1199-1101 cm⁻¹, respectively.



Scheme 1. Synthetic pathway of pyrazine-substituted benzamides. Reagents and Conditions: (i) HSO₃Cl, 10-15°C (till reaction completion), 80°C, stirring, 2 h; (ii) NH₂-R, acetone, reflux, 3-4 h; (iii) Thionyl chloride (SOCl₂), acetone, reflux, 3-4 h; (iv) 2-Amino-pyrazine, acetone, reflux, 3-4 h.

Peaks corresponding to SO₂NH stretching were observed around 3399-3001 cm⁻¹, confirming that these newly synthesized derivatives contain a sulphonamide moiety and a benzamide functional group. Stretching vibrations for the carbonyl group (C=O) were observed within the range of 1699-1601 cm⁻¹, indicating that these analogs contain a benzamide carbonyl

group in their structure. The occurrence of NH-bending vibrations near 1600 cm⁻¹ depicted the presence of an aromatic NH- moiety in the structure of these molecules.

Table 2. Physicochemical properties of the newly synthesized pyrazin-2-yl-substituted benzamide. derivatives.

Compound	R	Mol. Formula	M. Pt. (°C)	R _f [*]	% Yield
1	2-BrC ₆ H ₄	C ₁₇ H ₁₃ BrN ₄ O ₃ S	162-163	0.73	56
2	-C ₂ H ₅	C ₁₃ H ₁₄ N ₄ O ₃ S	142-143	0.55	52
3	-C ₄ H ₉	C ₁₅ H ₁₈ N ₄ O ₃ S	145-147	0.52	48
4	-OH	C ₁₁ H ₁₀ N ₄ O ₄ S	156-157	0.49	53
5	-NH ₂	C ₁₁ H ₁₁ N ₅ O ₃ S	156-158	0.68	45
6	-C ₆ H ₅	C ₁₇ H ₁₄ N ₄ O ₃ S	160-162	0.45	53
7	-H	C ₁₁ H ₁₀ N ₄ O ₃ S	150-152	0.59	57
8	2-ClC ₆ H ₄	C ₁₇ H ₁₃ ClN ₄ O ₃ S	165-167	0.61	55
9	-C ₃ H ₇	C ₁₄ H ₁₆ N ₄ O ₃ S	141-143	0.70	58
10	2-NO ₂ C ₆ H ₄	C ₁₇ H ₁₃ N ₅ O ₅ S	166-168	0.59	60
11	4-NO ₂ C ₆ H ₄	C ₁₇ H ₁₃ N ₅ O ₅ S	167-168	0.57	57
12	-NHC ₆ H ₅	C ₁₇ H ₁₅ N ₅ O ₃ S	156-158	0.42	61
13	-CH ₂ C ₆ H ₅	C ₁₈ H ₁₆ N ₄ O ₃ S	158-160	0.47	50

*TLC mobile phase: Toluene: Ethyl acetate (7:3).

3.3. *In vitro* GK assay.

The *in vitro* GK examination results illustrate how much the synthesized compounds activate the GK enzyme compared to the control (DMSO), as shown in Figure 1. Among the synthesized compounds tested, compounds 1, 8, and 9 demonstrated the most pronounced GK activity in the assay, showing a GK activation fold ranging from 1.9 to 2.10 compared to the control. Compounds 10, 11, 12, and 13 also exhibited significant activations of GK, with fold activation ranging from 1.48 to 1.86. On the other hand, compounds 3, 4, 5, and 6 displayed a poor level of GK activation, with a fold activation ranging from 1.27 to 1.37. Compounds 2 and 7 did not yield successful results in the *in vitro* GK assay. Among all the synthesized derivatives, molecule 8, which contains the N-2-chlorophenyl sulphonamide moiety, showed the greatest GK activity with a GK activation factor of 2.10. Compound 1, with a derivative containing an N-2-bromophenyl sulphonamide moiety, exhibited a significant 2.04-fold increase in activation compared to the control. Compound 8, with a derivative containing an N-2-chlorophenyl sulphonamide moiety, also showed a significant 2.04-fold increase in activation compared to the control.

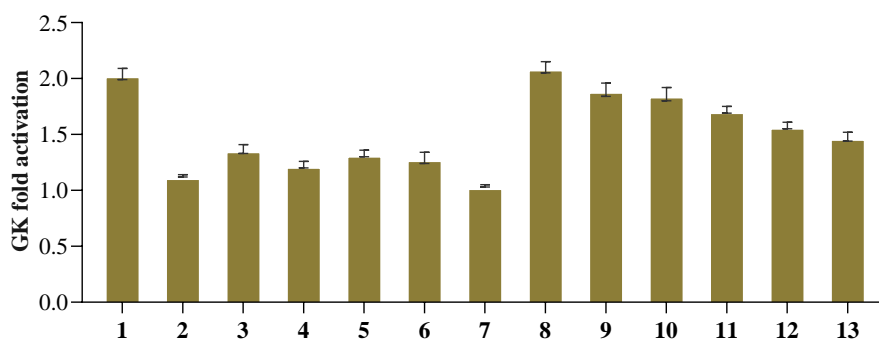


Figure 1. *In vitro* GK activation potential (fold activation of GK) of the designed pyrazine-substituted benzamide derivatives.

3.4. *In-vivo* study.

3.4.1. OGTT assay in normal rats.

After conducting a screening utilizing the *in vitro* GK assay, compounds 1, 8, and 9 were selected for further evaluation of their ability to reduce glucose levels using the OGTT

assay in normal rats, with metformin as the reference antidiabetic medication, the antihyperglycemic action was assessed by measuring blood glycaemic concentrations (mg/dL) at different time points (Figure 2) and calculating the glucose AUC (Figure 3). The findings from the antihyperglycemic activity testing showed that compound 8 exhibited higher effectiveness than compounds 1 and 9 in the OGTT experiment conducted on normal rats. Compound 8 demonstrated almost equal potency to the standard medication after 60 minutes and reduced blood glucose levels to the same extent as the standard drug after 120 minutes. Moreover, compound 8 exhibited a considerable reduction in glucose AUC relative to both the control and analogs, similar to that of the standard. The antihyperglycemic activity test findings demonstrated that compounds 1, 8, and 9 exhibited a comparable trend of blood glucose reduction to metformin. Compound 8 showed considerable efficacy in the in-vivo experiment compared to conventional metformin. Throughout the 120-minute duration of the OGTT assay, each compound tested for its antihyperglycemic effect successfully lowered blood glucose levels to an acceptable range. Importantly, no hypoglycemic effects were observed during the entire study period (0-120 minutes).

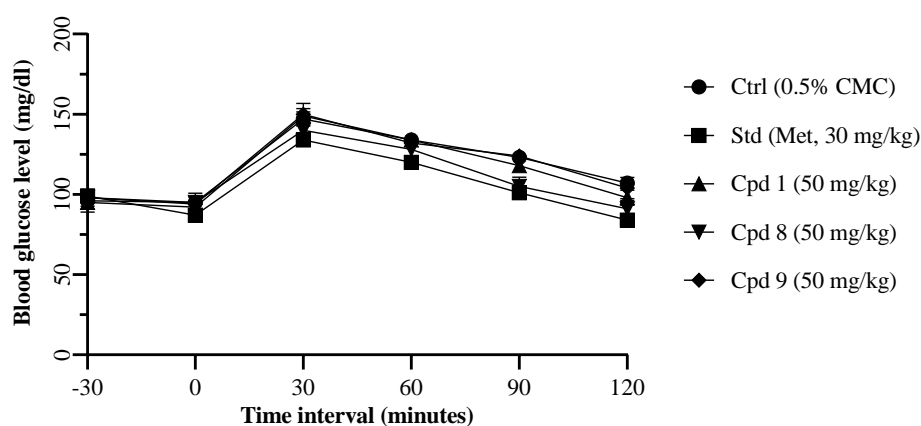


Figure 2. Effect of compounds 1, 8, and 9 on glycaemic content of blood at specified time intervals in normal rat OGTT model. Ctrl = Control (CMC) and Met = Metformin. All values are expressed as mean \pm standard deviation (n = 6).

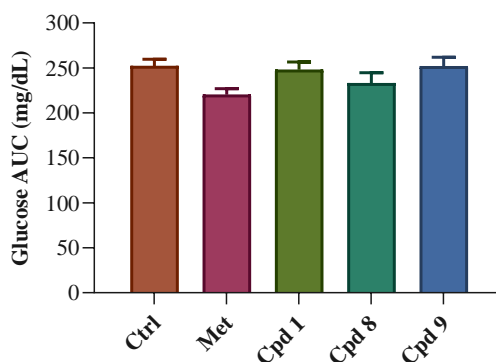


Figure 3. Glucose AUC reduction was exhibited by compounds 1, 8, and 9 in the OGTT model (normal rats). Ctrl = Control (Vehicle, i.e., CMC only) and Met = Metformin (Standard drug). All values are expressed as mean \pm standard deviation (n = 6).

3.4.2. OGTT assay in induced diabetic rats.

Compound 8 (25, 50, and 100 mg/kg body weight) was further evaluated for its antidiabetic properties by an OGTT test in alloxan-induced diabetic rats. Metformin, a common antidiabetic medicine, was used as a standard drug. The antidiabetic action was assessed by measuring glycaemic concentration in blood (in mg/dl) at different timing intervals (Figure 4).

Compound 8 displayed increased activity with an increase of the dose from 25 mg/kg to 100 mg/kg at 2, 4, and 6 h intervals. Compound 8 at 100 mg/kg (body weight) dose exhibited almost equal potency to the reference medication (i.e., metformin, 30 mg/kg body weight) at intervals of 2, 4, and 6 hours.

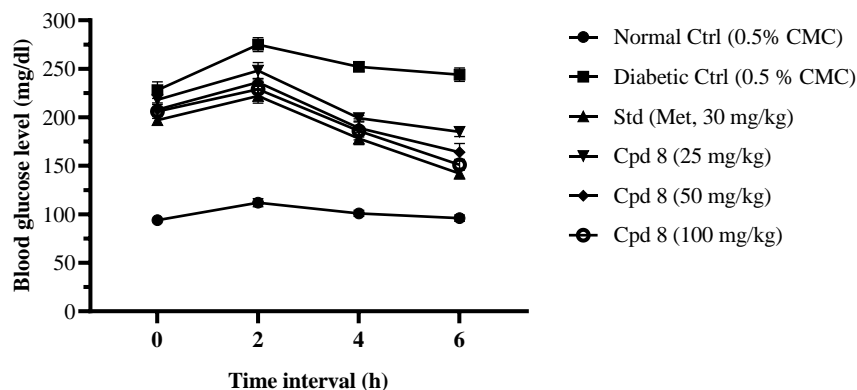


Figure 4. Effect of compound 8 on glycemic content of blood at specified time intervals in induced diabetic rat OGTT model. Ctrl = Control (CMC only) and Met = Metformin. All values are expressed as mean \pm standard deviation (n = 6).

3.5. *In silico* docking study.

In silico virtual screening is indeed a practical approach in drug discovery and various scientific fields to identify a secure and efficient remedy for major ailments, including T2DM. In this study, *in silico* molecular docking investigations were performed to discover the affinity and binding interactions of the designed GK activators using AutoDock Vina in the allosteric site of GK (PDB ID: 3IMX). The docking protocol used in this study was first validated by redocking the respective co-crystallized GK activator in the allosteric site of GK. The redocked GK activator produced a pose similar to that of the co-crystallized activator with the GK protein (Figure 5A) with a docking score (ΔG , kcal/mol) of -10.8 (PDB ID: 3IMX), indicating that a rational docking protocol was used in this study.

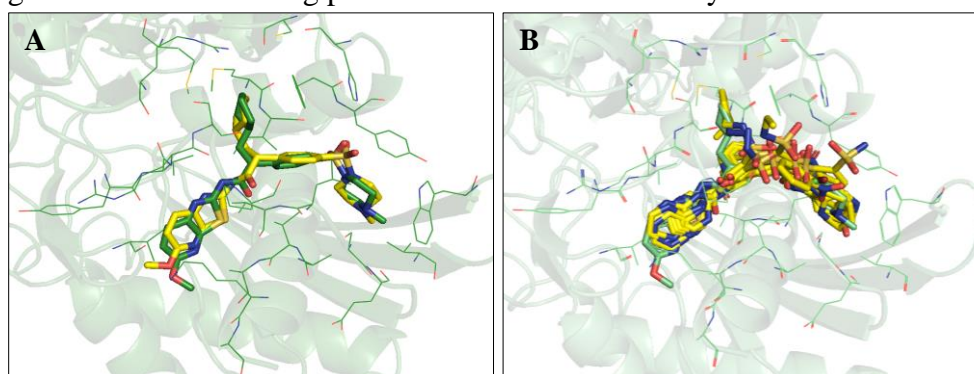


Figure 5. (A) The accuracy of the docking protocol was confirmed by conducting a redocking of the co-crystallized GK activator. The ligand that underwent redocking (yellow) exhibited a pose closely resembling that of the co-crystallized GK activator (green); (B) Overlay of the docked pose of the designed ligands (yellow) with that of the co-crystallized GK activator (green).

The designed compounds were docked in the allosteric site of human GK comprising Arg63, Ser69, Tyr215, Met210, Tyr214, Val452, and Val455 residues. Assessing the binding energy (ΔG) proves crucial in identifying potential drug candidates for various ailments. A molecule with lower binding energy indicates greater stability in the protein-ligand complex. The GK enzyme's allosteric region found a comparable binding pattern when the positioned design compounds were compared to the co-crystallized ligand (PDB ID: 3IMX), as depicted <https://nanobioletters.com/>

in Figure 5B. The molecular docking analyses indicated that these compounds have a complementary conformation when bound to the allosteric region of GK. Table 3 illustrates the docking score (ΔG) and the residues involved in hydrogen bonding and hydrophobic interactions.

Table 3. Illustration of docking scores (ΔG) and identifies the residues engaged in binding interactions of the designed compounds with the GK protein.

Ligand	ΔG	H-Bond Interactions		Hydrophobic interactions (residues involved)
		Residue	Distance (Å)	
1	-9.4	Arg63 Tyr214	2.24, 2.93 3.13	Pi-Sigma (Ile159); Pi-Alkyl (Arg63, Pro66, Trp99, Ile211, Leu451, Val455, Ala456, Lys459); Pi-Sulfur (Tyr214)
2	-7.7	Ser64 Pro66 Ser69 Tyr214	2.51 2.77 3.20 2.89	Pi-Pi T-shaped (Trp99, Tyr214); Pi-Alkyl (Val91, Leu451, Ala454, Val455); Pi-Sulfur (Tyr214)
3	-7.3	Tyr214	2.15	Pi-Sigma (Ile159); Pi-Alkyl (Arg63, Pro66, Ile211, Tyr214, Val455, Ala456, Lys459); Alkyl (Met210, Ile211)
4	-7.4	Arg63 Ile211	3.04 2.66, 2.69	Pi-Alkyl (Val62, Arg63, Pro66, Ile159, Val455, Ala456, Lys459); Pi-Sulfur (Tyr214)
5	-7.1	Ser64 Pro66 Tyr214	2.44, 2.40 2.41 2.56	Pi-Sigma (Ile159); Pi-Alkyl (Pro66, Ile211, Val455, Ala456, Lys459)
6	-8.4	-	-	Pi-Pi T-shaped (Trp99, Tyr215); Pi-Sigma (Val455); Pi-Alkyl (Val62, Pro66, Ile159, Ile211, Leu451, Ala454, Val455, Ala456); Pi-Sulfur (Tyr214)
7	-6.4	Trp99	2.81	Pi-Pi T-shaped (Trp99); Pi-Alkyl (Ile211, Val455); Pi-Sulfur (His218)
8	-9.3	Arg63 Leu451	3.13 3.09	Pi-Pi T-shaped (Trp99); Pi-Sigma (Ile211) Pi-Alkyl (Val62, Pro66, Ile159, Leu451, Val455, Ala456, Lys459); Pi-Sulfur (Tyr214)
9	-9.3	Arg63 Leu451	3.05 2.35	Pi-Sigma (Ile211); Pi-Alkyl (Val62, Pro66, Ile159, Val455, Ala456, Lys459); Alkyl (Leu451, Ala454, Val455); Pi-Sulfur (Tyr214)
10	-8.8	Arg63 Trp99	3.05 3.30	Pi-Sigma (Val455); Pi-Alkyl (Val62, Pro66, Ile159, Ile211, Ala454, Val455, Ala456); Pi-Sulfur (Tyr214)
11	-8.9	Ser69 Tyr214	3.16 3.31	Pi-Pi T-shaped (Trp99, Tyr215); Pi-Sigma (Val455); Pi-Alkyl (Val62, Pro66, Ile159, Ile211, Leu451, Val455, Ala456, Lys459); Pi-Sulfur (Tyr214)
12	-9.2	Arg63 Tyr214	2.38, 3.33 2.53	Pi-Cation (Tyr214); Pi-Pi Stacked (Tyr214) Pi-Sigma (Met235, Val455); Pi-Alkyl (Arg63, Pro66, Ile159, Ile211, Val452, Lys459)
13	-9.1	Arg63 Leu451	3.04 3.07	Pi-Pi T-Shaped (Trp99, Tyr215); Pi-Alkyl (Val62, Arg63, Pro66, Val91, Ile159, Ile211, Leu451, Ala454, Val455, Ala456, Lys459); Pi-Sulfur (Tyr214)

Compound 1 underwent a detailed analysis to elucidate its binding interactions with the allosteric site residues of the GK protein (Figure 6). In the docking of compound 1 with the GK protein, notable interactions were observed. Specifically, three hydrogen bonds were identified: one between the C=O group of the GK's Arg63 residue and the NH group of the CONH moiety (bond distance: 2.24 Å), another involving the NH group of GK's Arg63 residue and the N atom of the pyrazine-2-yl ring (2.93 Å), and a third linking the OH group of GK's Tyr214 residue with the S=O group of the SO₂NH moiety (3.13 Å). Compound 1 exhibited hydrophobic interactions within GK's allosteric site, involving Pi-Sigma interactions (between the pyrazin-2-yl ring and Ile159 residue), Pi-Alkyl interactions (involving the pyrazin-2-yl ring with Arg63, Pro66, Trp99, Ile211, Leu451, Val455, Ala456, Lys459 residues; the bromo group of the 2-bromophenyl ring with Trp99 residue; the central phenyl ring or benzamide scaffold

with Ile211 and Val455 residues; and the 2-bromophenyl ring with Leu451 and Val 455 residues), and Pi-Sulfur interactions (between the sulfur of the SO₂NH moiety and Tyr214 residue). These diverse interactions contribute to the robust binding and stability of compound 1 within the allosteric site of the GK protein.

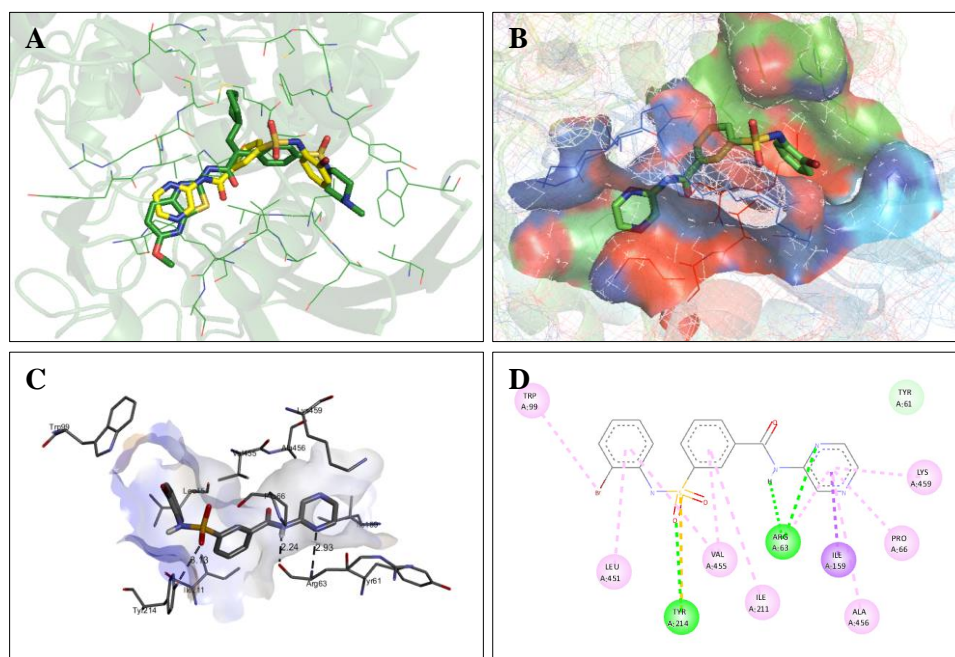


Figure 6. Interaction analysis of compound 1 with GK. (A) Superimposition of the docked pose of Compound 1 (yellow sticks) with that of the co-crystallized GK activator (green sticks); (B) Orientation of the compound 1 in the allosteric site within the GK protein; (C) Compound 1 in a 3D docked pose illustrating hydrogen bond interactions; (D) 2D docked pose of compound 1 showing hydrogen bonds (green dashes) and hydrophobic interactions (pink & purple dashes) with the GK protein.

3.6. *In silico* toxicity evaluation.

The newly designed derivatives' possible toxicity (mutagenic, carcinogenic, cardiotoxicity, immunotoxicity, skin irritation, and reproductive toxicity) was accessed using the pkCSM online tool (Table 4). pkCSM is an openly available online tool that uses graph-based markers to efficiently assess small compounds' pharmacokinetic and toxicity characteristics [68-69]. Compounds 10 and 11 were forecasted for mutagenicity (AMES toxicity), while hepatotoxicity was predicted for all the designed compounds, excluding compound 7. Additionally, compounds 1, 6, 8, 10, 11, and 12 were predicted to have cardiac toxicity (hERG II inhibition). The 1.709 to 2.769 mol/kg range was predicted for oral rat acute toxicity (LD₅₀). Chronic oral rat toxicity was predicted to be between 1.224 and 1.892 log mg/kg_bw/day. It was predicted that the maximum amount (of designed compounds) that humans might tolerate would be between 0.015 and 0.780 log mg/kg/day. A prior evaluation that is carried out *in silico* may be a useful supplement to future investigations on the potential dangers of compounds.

Table 4. Predicted toxicity probability (presence or absence) for the designed compounds via pkCSM analysis.

Compound	AMES toxicity	Max. tolerated dose	hERG I inhibition	hERG II inhibition	Rat acute tox.	Rat chronic tox.	Hepato-toxicity	Skin toxicity
1	No	0.214	No	Yes	2.337	1.224	Yes	No
2	No	0.695	No	No	2.339	1.670	Yes	No
3	No	0.780	No	No	2.319	1.742	Yes	No
4	No	0.751	No	No	2.769	1.730	Yes	No
5	No	0.730	No	No	2.760	1.756	Yes	No

Compound	AMES toxicity	Max. tolerated dose	hERG I inhibition	hERG II inhibition	Rat acute tox.	Rat chronic tox.	Hepato-toxicity	Skin toxicity
6	No	0.015	No	Yes	2.366	1.238	Yes	No
7	No	0.517	No	No	1.709	1.231	No	No
8	No	0.216	No	Yes	2.323	1.240	Yes	No
9	No	0.721	No	No	2.380	1.684	Yes	No
10	Yes	0.053	No	Yes	2.549	1.709	Yes	No
11	Yes	0.027	No	Yes	2.630	1.892	Yes	No
12	No	0.238	No	No	2.298	1.498	Yes	No
13	No	0.209	No	No	2.254	1.299	Yes	No

AMES Toxicity: Mutagenic or carcinogenic potential; Max. Tolerated Dose: Maximum tolerated human dose (log mg/kg/day); hERG I inhibition: hERG I inhibition (cardiotoxicity); hERG II inhibition: hERG II inhibition (cardiotoxicity); Rat Acute Tox.: Oral rat acute toxicity (LD50) (mol/kg); Rat Chronic Tox.: Oral rat chronic toxicity (log mg/kg_bw/day); Skin Toxicity: Skin sensitization.

4. Conclusions

In conclusion, this study focused on the design, synthesis, and evaluation of novel pyrazine-substituted benzamides as potential activators of human GK for the treatment of T2DM. The synthesized compounds underwent comprehensive assessments, including *in vitro* enzymatic tests, computer-based docking analyses, and *in vivo* experiments. Compounds 1, 8, and 9 emerged as the most potent GK activators *in vitro*, exhibiting activation fold values between 1.90 and 2.10. Following OGTT in healthy rats, compounds 1 and 8 demonstrated promising antihyperglycemic effects, consistent with both *in vitro* results and docking studies. *In vivo*, evaluation of compound 8 revealed remarkable efficacy in lowering blood glucose levels during OGTT in healthy rats, comparable to the standard diabetes drug metformin. Moreover, computational docking analyses provided insights into the interactions between the designed compounds and residues in the allosteric site of GK, supporting the alignment of *in silico* predictions with experimental results. These findings underscore the potential of the newly developed pyrazine-substituted benzamides as promising candidates for GK activators, characterized by their demonstrated safety, efficacy, and oral bioavailability, making them viable therapeutic options for T2DM management.

Author Contributions

All authors have read and agreed to the published version of the manuscript.

Institutional Review Board Statement

Not applicable.

Informed Consent Statement

Not applicable.

Data Availability Statement

Data supporting the findings of this study are available upon reasonable request from the corresponding author.

Funding

This research received no external funding.

Acknowledgments

The authors are thankful to Chitkara College of Pharmacy, Chitkara University (Punjab), and C.S.I.R.- Institute of Himalayan Bioresource Technology (IHBT), Palampur, for their support and encouragement for this research work.

Conflicts of Interest

The authors declare no conflict of interest.

References

1. Magliano, D.J.; Boyko, E.J. IDF Diabetes Atlas, 10th Edition; International Diabetes Federation: Brussels, **2021**.
2. Dagogo-Jack, S. Diabetes Mellitus in Developing Countries and Underserved Communities. Springer International: Switzerland, **2017**; <https://doi.org/10.1007/978-3-319-41559-8>.
3. Grewal, A.S.; Kharb, R.; Prasad, D.N.; Dua, J.S.; Lather, V. *N*-pyridin-2-yl benzamide analogues as allosteric activators of glucokinase: Design, synthesis, in vitro, in silico and in vivo evaluation. *Chem. Biol. Drug Des.* **2019**, *93*, 364-372, <http://doi.org/10.1111/cbdd.13423>.
4. Sharma, P.; Singh, S.; Sharma, N.; Singla, D.; Guarve, K.; Grewal, A.S. Targeting human Glucokinase for the treatment of type 2 diabetes: an overview of allosteric Glucokinase activators. *J. Diabetes Metab. Disord.* **2022**, *21*, 1129-1137, <https://doi.org/10.1007/s40200-022-01019-x>.
5. Dhankhar, S.; Chauhan, S.; Mehta, D.K.; Nitika; Saini, K.; Saini, M.; Das, R.; Gupta, S.; Gautam, V. Novel targets for potential therapeutic use in Diabetes mellitus. *Diabetes Metab. Syndr.* **2023**, *15*, 17, <https://doi.org/10.1186/s13098-023-00983-5>.
6. American Diabetes Association Professional Practice, C. 2. *Diagnosis and Classification of Diabetes: Standards of Care in Diabetes—2024. Diabetes Care* **2023**, *47*, S20-S42, <https://doi.org/10.2337/dc24-S002>.
7. Kumar, S.; Behl, T.; Sachdeva, M.; Sehgal, A.; Kumari, S.; Kumar, A.; Kaur, G.; Yadav, H.N.; Bungau, S. Implicating the effect of ketogenic diet as a preventive measure to obesity and diabetes mellitus. *Life Sci.* **2021**, *264*, 118661, <https://doi.org/10.1016/j.lfs.2020.118661>.
8. Arora, A.; Behl, T.; Sehgal, A.; Singh, S.; Sharma, N.; Bhatia, S.; Sobarzo-Sanchez, E.; Bungau, S. Unravelling the involvement of gut microbiota in type 2 diabetes mellitus. *Life Sci.* **2021**, *273*, 119311, <https://doi.org/10.1016/j.lfs.2021.119311>.
9. Ghusn, W.; Hurtado, M.D.; Acosta, A. Weight-centric treatment of type 2 diabetes mellitus. *Obesity Pillars* **2022**, *4*, 100045, <https://doi.org/10.1016/j.obpill.2022.100045>.
10. Gawli, K.; Bojja, K.S. Molecules and targets of antidiabetic interest. *Phytomed. Plus* **2024**, *4*, 100506, <https://doi.org/10.1016/j.phyplu.2023.100506>.
11. Grewal, A.S.; Lather, V.; Charaya, N.; Sharma, N.; Singh, S.; Kairys, V. Recent developments in medicinal chemistry of allosteric activators of human glucokinase for type 2 diabetes mellitus therapeutics. *Curr. Pharm. Des.* **2020**, *26*, 2510-2552, <https://doi.org/10.2174/1381612826666200414163148>.
12. Grewal, A.S.; Lather, V. Small molecule allosteric activators of human glucokinase for the treatment of type 2 diabetes: current status and challenges. *Curr. Drug Discov. Technol.* **2022**, *19*, e160422203687, <https://doi.org/10.2174/1570163819666220416212906>.
13. Yang, W.; Wu, H.; Cai, X.; Lin, C.; Jiao, R.; Ji, L. Evaluation of efficacy and safety of glucokinase activators—a systematic review and meta-analysis. *Front. Endocrinol.* **2023**, *14*, 1175198, <https://doi.org/10.3389/fendo.2023.1175198>.
14. McKerrecher, D.; Allen, J.V.; Bowker, S.S.; Boyd, S.; Caulkett, P.W.R.; Currie, G.S.; Davies, C.D.; Fenwick, M.L.; Gaskin, H.; Grange, E.; Hargreaves, R.B.; Hayter, B.R.; James, R.; Johnson, K.M.; Johnstone, C.; Jones, C.D.; Lackie, S.; Rayner, J.W.; Walker, R.P. Discovery, synthesis and biological evaluation of novel glucokinase activators. *Bioorg. Med. Chem. Lett.* **2005**, *15*, 2103-2106, <https://doi.org/10.1016/j.bmcl.2005.01.087>.
15. Iino, T.; Tsukahara, D.; Kamata, K.; Sasaki, K.; Ohyama, S.; Hosaka, H.; Hasegawa, T.; Chiba, M.; Nagata, Y.; Eiki, J.-i.; Nishimura, T. Discovery of potent and orally active 3-alkoxy-5-phenoxy-*N*-thiazolyl benzamides as novel allosteric glucokinase activators. *Bioorg. Med. Chem.* **2009**, *17*, 2733-2743, <https://doi.org/10.1016/j.bmc.2009.02.038>.

16. Iino, T.; Hashimoto, N.; Sasaki, K.; Ohyama, S.; Yoshimoto, R.; Hosaka, H.; Hasegawa, T.; Chiba, M.; Nagata, Y.; Eiki, J.-i.; Nishimura, T. Structure–activity relationships of 3,5-disubstituted benzamides as glucokinase activators with potent in vivo efficacy. *Bioorg. Med. Chem.* **2009**, *17*, 3800-3809, <https://doi.org/10.1016/j.bmc.2009.04.040>.
17. Iino, T.; Hashimoto, N.; Hasegawa, T.; Chiba, M.; Eiki, J.-i.; Nishimura, T. Metabolic activation of *N*-thiazol-2-yl benzamide as glucokinase activators: Impacts of glutathione trapping on covalent binding. *Bioorg. Med. Chem. Lett.* **2010**, *20*, 1619-1622, <https://doi.org/10.1016/j.bmcl.2010.01.041>.
18. Pike, K.G.; Allen, J.V.; Caulkett, P.W.R.; Clarke, D.S.; Donald, C.S.; Fenwick, M.L.; Johnson, K.M.; Johnstone, C.; McKerrecher, D.; Rayner, J.W.; Walker, R.P.; Wilson, I. Design of a potent, soluble glucokinase activator with increased pharmacokinetic half-life. *Bioorg. Med. Chem. Lett.* **2011**, *21*, 3467-3470, <https://doi.org/10.1016/j.bmcl.2011.03.093>.
19. Bowler, J.M.; Hervert, K.L.; Kearley, M.L.; Miller, B.G. Small-Molecule Allosteric Activation of Human Glucokinase in the Absence of Glucose. *ACS Med. Chem. Lett.* **2013**, *4*, 580-584, <https://doi.org/10.1021/ml400061x>.
20. Li, C.; Zhang, Y.; Chen, L.; Li, X. Glucokinase and glucokinase activator. *Life Metab.* **2023**, *2*, load031, <https://doi.org/10.1093/lifemeta/load031>.
21. Park, K.; Lee, B.M.; Hyun, K.H.; Lee, D.H.; Choi, H.H.; Kim, H.; Chong, W.; Kim, K.B.; Nam, S.Y. Discovery of 3-(4-methanesulfonylphenoxy)-*N*-[1-(2-methoxy-ethoxymethyl)-1*H*-pyrazol-3-yl]-5-(3-methylpyridin-2-yl)-benzamide as a novel glucokinase activator (GKA) for the treatment of type 2 diabetes mellitus. *Bioorg. Med. Chem.* **2014**, *22*, 2280-2293, <https://doi.org/10.1016/j.bmc.2014.02.009>.
22. Park, K.; Lee, B.M.; Hyun, K.H.; Han, T.; Lee, D.H.; Choi, H.H. Design and Synthesis of Acetylenyl Benzamide Derivatives as Novel Glucokinase Activators for the Treatment of T2DM. *ACS Med. Chem. Lett.* **2015**, *6*, 296-301, <https://doi.org/10.1021/ml5004712>.
23. Singh, R.; Lather, V.; Pandita, D.; Judge, V.; N Arumugam, K.; Singh Grewal, A. Synthesis, Docking and Antidiabetic Activity of Some Newer Benzamide Derivatives as Potential Glucokinase Activators. *Lett. Drug Des. Discov.* **2017**, *14*, 540-553, <https://doi.org/10.2174/1570180813666160819125342>.
24. Charaya, N.; Pandita, D.; Grewal, A.S.; Lather, V. Design, synthesis and biological evaluation of novel thiazol-2-yl benzamide derivatives as glucokinase activators. *Comput. Biol. Chem.* **2018**, *73*, 221-229, <https://doi.org/10.1016/j.compbiolchem.2018.02.018>.
25. Grewal, A.S.; Kharb, R.; Dua, J.S.; Lather, V. Molecular docking assessment of *N*-heteroaryl substituted benzamide derivatives as glucokinase activators. *Asian J. Pharm. Pharmacol.* **2019b** **2019**, *5*, 129-136, <https://doi.org/10.31024/ajpp.2019.5.1.18>.
26. Grewal, A.S.; Sharma, K.; Singh, S.; Singh, V.; Pandita, D.; Lather, V. Design, synthesis and antidiabetic activity of novel sulfamoyl benzamide derivatives as glucokinase activators. *J. Pharm. Technol. Res.* **2018**, *6*, 115-124, <https://doi.org/10.15415/jptrm.2018.62008>.
27. Grewal, A.S.; Kharb, R.; Prasad, D.N.; Dua, J.S.; Lather, V. *N*-pyridin-2-yl benzamide analogues as allosteric activators of glucokinase: Design, synthesis, in vitro, in silico and in vivo evaluation. *Chem. Biol. Drug Des.* **2019**, *93*, 364-372, <https://doi.org/10.1111/cbdd.13423>.
28. Grewal, A.S.; Kharb, R.; Prasad, D.N.; Dua, J.S.; Lather, V. Design, synthesis and evaluation of novel 3,5-disubstituted benzamide derivatives as allosteric glucokinase activators. *BMC Chem.* **2019**, *13*, 2, <https://doi.org/10.1186/s13065-019-0532-8>.
29. Singh, S.; Arora, S.; Dhalio, E.; Sharma, N.; Arora, K.; Grewal, A.S. Design and synthesis of newer *N*-benzimidazol-2-yl benzamide analogues as allosteric activators of human glucokinase. *Med. Chem. Res.* **2021**, *30*, 760-770, <https://doi.org/10.1007/s00044-020-02697-z>.
30. Arora, S.; Grewal, A.S.; Sharma, N.; Arora, K.; Dhalio, E.; Singh, S. Design, synthesis, and evaluation of some novel *N*-benzothiazol-2-yl benzamide derivatives as allosteric activators of human glucokinase. *J. Appl. Pharm. Sci.* **2021**, *11*, 038-047, <https://doi.org/0.7324/JAPS.2021.11s104>.
31. Behera, P.M.; Behera, D.K.; Satpati, S.; Agnihotri, G.; Nayak, S.; Padhi, P.; Dixit, A. Molecular modeling and identification of novel glucokinase activators through stepwise virtual screening. *J. Mol. Graph. Model.* **2015**, *57*, 122-130, <https://doi.org/10.1016/j.jmkgm.2015.01.012>.
32. Sharma, R.; Litchfield, J.; Bergman, A.; Atkinson, K.; Kazierad, D.; Gustavson, S.M.; Di, L.; Pfefferkorn, J.A.; Kalgutkar, A.S. Comparison of the Circulating Metabolite Profile of PF-04991532, a Hepatoselective Glucokinase Activator, Across Preclinical Species and Humans: Potential Implications in Metabolites in Safety Testing Assessment. *Drug Metab. Dispos.* **2015**, *43*, 190-198, <https://doi.org/10.1124/dmd.114.061218>.

33. de Assis, T.M.; Gajo, G.C.; de Assis, L.C.; Garcia, L.S.; Silva, D.R.; Ramalho, T.C.; da Cunha, E.F.F. QSAR Models Guided by Molecular Dynamics Applied to Human Glucokinase Activators. *Chem. Biol. Drug Des.* **2016**, *87*, 455-466, <https://doi.org/10.1111/cbdd.12683>.
34. Deshpande, A.M.; Bhuniya, D.; De, S.; Dave, B.; Vyavahare, V.P.; Kurhade, S.H.; Kandalkar, S.R.; Naik, K.P.; Kobal, B.S.; Kaduskar, R.D.; Basu, S.; Jain, V.; Patil, P.; Chaturvedi Joshi, S.; Bhat, G.; Rajee, A.A.; Reddy, S.; Gundu, J.; Madgula, V.; Tambe, S.; Shitole, P.; Umrani, D.; Chugh, A.; Palle, V.P.; Mookhtiar, K.A. Discovery of liver-directed glucokinase activator having anti-hyperglycemic effect without hypoglycemia. *Eur. J. Med. Chem.* **2017**, *133*, 268-286, <https://doi.org/10.1016/j.ejmech.2017.03.042>.
35. Xu, J.; Lin, S.; Myers, R.W.; Trujillo, M.E.; Pachanski, M.J.; Malkani, S.; Chen, H.-s.; Chen, Z.; Campbell, B.; Eiermann, G.J.; Elowe, N.; Farrer, B.T.; Feng, W.; Fu, Q.; Kats-Kagan, R.; Kavana, M.; McMasters, D.R.; Mitra, K.; Tong, X.; Xu, L.; Zhang, F.; Zhang, R.; Addona, G.H.; Berger, J.P.; Zhang, B.; Parmee, E.R. Discovery of orally active hepatoselective glucokinase activators for treatment of Type II Diabetes Mellitus. *Bioorg. Med. Chem. Lett.* **2017**, *27*, 2063-2068, <https://doi.org/10.1016/j.bmcl.2016.10.088>.
36. Cheruvallath, Z.S.; Gwaltney, S.L.; Sabat, M.; Tang, M.; Wang, H.; Jennings, A.; Hosfield, D.; Lee, B.; Wu, Y.; Halkowycz, P.; Grimshaw, C.E. Discovery of potent and orally active 1,4-disubstituted indazoles as novel allosteric glucokinase activators. *Bioorg. Med. Chem. Lett.* **2017**, *27*, 2678-2682, <https://doi.org/10.1016/j.bmcl.2017.04.041>.
37. Sidduri, A.; Grimsby, J.S.; Corbett, W.L.; Sarabu, R.; Grippo, J.F.; Lou, J.; Kester, R.F.; Dvorozniak, M.; Marcus, L.; Spence, C.; Racha, J.K.; Moore, D.J. 2,3-Disubstituted acrylamides as potent glucokinase activators. *Bioorg. Med. Chem. Lett.* **2010**, *20*, 5673-5676, <https://doi.org/10.1016/j.bmcl.2010.08.029>.
38. Takahashi, K.; Hashimoto, N.; Nakama, C.; Kamata, K.; Sasaki, K.; Yoshimoto, R.; Ohyama, S.; Hosaka, H.; Maruki, H.; Nagata, Y.; Eiki, J.-i.; Nishimura, T. The design and optimization of a series of 2-(pyridin-2-yl)-1*H*-benzimidazole compounds as allosteric glucokinase activators. *Bioorg. Med. Chem.* **2009**, *17*, 7042-7051, <https://doi.org/10.1016/j.bmc.2009.05.037>.
39. Santos-Ballardo, C.L.; Montes-Ávila, J.; Rendon-Maldonado, J.G.; Ramos-Payan, R.; Montaña, S.; Sarmiento-Sánchez, J.I.; Acosta-Cota, S.d.J.; Ochoa-Terán, A.; Bastidas-Bastidas, P.d.J.; Osuna-Martínez, U. Design, synthesis, *in silico*, and *in vitro* evaluation of benzylbenzimidazolone derivatives as potential drugs on α -glucosidase and glucokinase as pharmacological targets. *RSC Adv.* **2023**, *13*, 21153-21162, <https://doi.org/10.1039/d3ra02916f>.
40. Iino, T.; Sasaki, Y.; Bamba, M.; Mitsuya, M.; Ohno, A.; Kamata, K.; Hosaka, H.; Maruki, H.; Futamura, M.; Yoshimoto, R.; Ohyama, S.; Sasaki, K.; Chiba, M.; Ohtake, N.; Nagata, Y.; Eiki, J.-i.; Nishimura, T. Discovery and structure-activity relationships of a novel class of quinazoline glucokinase activators. *Bioorg. Med. Chem. Lett.* **2009**, *19*, 5531-5538, <https://doi.org/10.1016/j.bmcl.2009.08.064>.
41. Song, H.-p.; Tian, K.; Lei, L.; Shen, Z.-f.; Liu, S.-x.; Zhang, L.-j.; Song, H.-r.; Jin, X.-f.; Feng, Z.-q. Novel *N*-(pyrimidin-4-yl)thiazol-2-amine derivatives as dual-action hypoglycemic agents that activate GK and PPAR γ . *Acta Pharm. Sin. B* **2011**, *1*, 166-171, <https://doi.org/10.1016/j.apsb.2011.07.002>.
42. Hinklin, R.J.; Boyd, S.A.; Chicarelli, M.J.; Condroski, K.R.; DeWolf, W.E., Jr.; Lee, P.A.; Lee, W.; Singh, A.; Thomas, L.; Voegtli, W.C.; Williams, L.; Aicher, T.D. Identification of a New Class of Glucokinase Activators through Structure-Based Design. *J. Med. Chem.* **2013**, *56*, 7669-7678, <https://doi.org/10.1021/jm401116k>.
43. Bonn, P.; Brink, D.M.; Fägerhag, J.; Jurva, U.; Robb, G.R.; Schnecke, V.; Svensson Henriksson, A.; Waring, M.J.; Westerlund, C. The discovery of a novel series of glucokinase activators based on a pyrazolopyrimidine scaffold. *Bioorg. Med. Chem. Lett.* **2012**, *22*, 7302-7305, <https://doi.org/10.1016/j.bmcl.2012.10.090>.
44. Filipski, K.J.; Guzman-Perez, A.; Bian, J.; Perreault, C.; Aspnes, G.E.; Didiuk, M.T.; Dow, R.L.; Hank, R.F.; Jones, C.S.; Maguire, R.J.; Tu, M.; Zeng, D.; Liu, S.; Knafels, J.D.; Litchfield, J.; Atkinson, K.; Derksen, D.R.; Bourbonais, F.; Gajiwala, K.S.; Hickey, M.; Johnson, T.O.; Humphries, P.S.; Pfefferkorn, J.A. Pyrimidone-based series of glucokinase activators with alternative donor-acceptor motif. *Bioorg. Med. Chem. Lett.* **2013**, *23*, 4571-4578, <https://doi.org/10.1016/j.bmcl.2013.06.036>.
45. Castelhana, A.L.; Dong, H.; Fyfe, M.C.T.; Gardner, L.S.; Kamikozawa, Y.; Kurabayashi, S.; Nawano, M.; Ohashi, R.; Procter, M.J.; Qiu, L.; Rasamison, C.M.; Schofield, K.L.; Shah, V.K.; Ueta, K.; Williams, G.M.; Witter, D.; Yasuda, K. Glucokinase-activating ureas. *Bioorg. Med. Chem. Lett.* **2005**, *15*, 1501-1504, <https://doi.org/10.1016/j.bmcl.2004.12.083>.
46. Zhang, L.; Tian, K.; Li, Y.; Lei, L.; Qin, A.; Zhang, L.; Song, H.; Huo, L.; Zhang, L.; Jin, X.; Shen, Z.; Feng, Z. Novel phenyl-urea derivatives as dual-target ligands that can activate both GK and PPAR γ . *Acta Pharm. Sin. B* **2012**, *2*, 588-597, <https://doi.org/10.1016/j.apsb.2012.10.002>.

47. Du, X.; Hinklin, R.J.; Xiong, Y.; Dransfield, P.; Park, J.; Kohn, T.J.; Pattaropong, V.; Lai, S.; Fu, Z.; Jiao, X.; Chow, D.; Jin, L.; Davda, J.; Veniant, M.M.; Anderson, D.A.; Baer, B.R.; Bencsik, J.R.; Boyd, S.A.; Chicarelli, M.J.; Mohr, P.J.; Wang, B.; Condroski, K.R.; DeWolf, W.E.; Conn, M.; Tran, T.; Yang, J.; Aicher, T.D.; Medina, J.C.; Coward, P.; Houze, J.B. C5-Alkyl-2-methylurea-Substituted Pyridines as a New Class of Glucokinase Activators. *ACS Med. Chem. Lett.* **2014**, *5*, 1284-1289, <https://doi.org/10.1021/ml500341w>.
48. Li, Y.; Tian, K.; Qin, A.; Zhang, L.; Huo, L.; Lei, L.; Shen, Z.; Song, H.; Feng, Z. Discovery of novel urea derivatives as dual-target hypoglycemic agents that activate glucokinase and PPAR γ . *Eur. J. Med. Chem.* **2014**, *76*, 182-192, <https://doi.org/10.1016/j.ejmech.2014.02.024>.
49. Hinklin, R.J.; Aicher, T.D.; Anderson, D.A.; Baer, B.R.; Boyd, S.A.; Condroski, K.R.; DeWolf, W.E., Jr.; Kraser, C.F.; McVean, M.; Rhodes, S.P.; Sturgis, H.L.; Voegtli, W.C.; Williams, L.; Houze, J.B. Discovery of 2-Pyridylureas as Glucokinase Activators. *J. Med. Chem.* **2014**, *57*, 8180-8186, <https://doi.org/10.1021/jm501204z>.
50. Dransfield, P.J.; Pattaropong, V.; Lai, S.; Fu, Z.; Kohn, T.J.; Du, X.; Cheng, A.; Xiong, Y.; Komorowski, R.; Jin, L.; Conn, M.; Tien, E.; DeWolf, W.E., Jr.; Hinklin, R.J.; Aicher, T.D.; Kraser, C.F.; Boyd, S.A.; Voegtli, W.C.; Condroski, K.R.; Veniant-Ellison, M.; Medina, J.C.; Houze, J.; Coward, P. Novel Series of Potent Glucokinase Activators Leading to the Discovery of AM-2394. *ACS Med. Chem. Lett.* **2016**, *7*, 714-718, <https://doi.org/10.1021/acsmchemlett.6b00140>.
51. Semenov, A.V.; Tarasova, I.V.; Khramov, V.S.; Semenova, E.V.; Inchina, V.I.; Vakaeva, S.S. Glucokinase Activators Based on *N*-Aryl-*N'*-Pyridin-2-Ylurea Derivatives. *Pharm. Chem. J.* **2018**, *52*, 209-212, <https://doi.org/10.1007/s11094-018-1792-7>.
52. Vella, A.; Freeman, J.L.R.; Dunn, I.; Keller, K.; Buse, J.B.; Valcarce, C. Targeting hepatic glucokinase to treat diabetes with TTP399, a hepatoselective glucokinase activator. *Sci. Transl. Med.* **2019**, *11*, eaau3441, <https://doi.org/10.1126/scitranslmed.aau3441>.
53. Egan, A.; Vella, A. TTP399: an investigational liver-selective glucokinase (GK) activator as a potential treatment for type 2 diabetes. *Expert Opin. Investig. Drugs* **2019**, *28*, 741-747, <https://doi.org/10.1080/13543784.2019.1654993>.
54. Daina, A.; Michielin, O.; Zoete, V. SwissADME: a free web tool to evaluate pharmacokinetics, drug-likeness and medicinal chemistry friendliness of small molecules. *Sci. Rep.* **2017**, *7*, 42717, <https://doi.org/10.1038/srep42717>.
55. Lipinski, C.A.; Lombardo, F.; Dominy, B.W.; Feeney, P.J. Experimental and computational approaches to estimate solubility and permeability in drug discovery and development settings. *Adv. Drug Deliv. Rev.* **2001**, *46*, 3-26, [https://doi.org/10.1016/s0169-409x\(00\)00129-0](https://doi.org/10.1016/s0169-409x(00)00129-0).
56. Thakral, S.; Singh, V. (2019). 2,4-Dichloro-5-[(N-aryl/alkyl)sulfamoyl]benzoic acid derivatives: in vitro antidiabetic activity, molecular modeling and in silico ADMET screening. *Med. Chem.* **2019**, *15*(2), 186-195. <https://doi.org/10.2174/1573406414666180924164327>.
57. Grewal, A.S.; Lather, V.; Pandita, D.; Bhayana, G. Synthesis, Docking and Evaluation of Phenylacetic Acid and Trifluoro-methylphenyl Substituted Benzamide Derivatives as Potential PPAR δ Agonists. *Lett. Drug Des. Discov.* **2017**, *14*, 1239-1251, <https://doi.org/10.2174/1570180814666170327164443>.
58. Ahmed, M.F.; Kazim, S.M.; Ghori, S.S.; Mehjabeen, S.S.; Ahmed, S.R.; Ali, S.M.; Ibrahim, M. Antidiabetic Activity of *Vinca rosea* Extracts in Alloxan-Induced Diabetic Rats. *Int. J. Endocrinol.* **2010**, *2010*, 841090, <https://doi.org/10.1155/2010/841090>.
59. Chauhan, A.; Grewal, A.S.; Pandita, D.; Lather, V. Novel Cinnamic Acid Derivatives as Potential PPAR δ Agonists for Metabolic Syndrome: Design, Synthesis, Evaluation and Docking Studies. *Curr. Drug Discov. Technol.* **2020**, *17*, 338-347, <https://doi.org/10.2174/1570163816666190314124543>.
60. Trott, O.; Olson, A.J. AutoDock Vina: Improving the speed and accuracy of docking with a new scoring function, efficient optimization, and multithreading. *J. Comput. Chem.* **2010**, *31*, 455-461, <https://doi.org/10.1002/jcc.21334>.
61. Morris, G.M.; Huey, R.; Lindstrom, W.; Sanner, M.F.; Belew, R.K.; Goodsell, D.S.; Olson, A.J. AutoDock4 and AutoDockTools4: Automated docking with selective receptor flexibility. *J. Comput. Chem.* **2009**, *30*, 2785-2791, <https://doi.org/10.1002/jcc.21256>.
62. Miteva, M.A.; Guyon, F.; Tuffi $\frac{1}{2}$ ry, P. Frog2: Efficient 3D conformation ensemble generator for small compounds. *Nucleic Acids Res.* **2010**, *38*, W622-W627, <https://doi.org/10.1093/nar/gkq325>.
63. Rani, J.; Jagta, N.; Deswal, G.; Chopra, B.; Dhingra, A.K.; Guarve, K.; Grewal, A.S. Molecular docking-guided screening of phytoconstituents from *Artemisia princeps* as Allosteric Glucokinase Activators. *Chem. Biol. Lett.* **2023**, *10*, 547, <https://doi.org/10.21203/rs.3.rs-2178001/v1>.

64. Kaur, A.; Thakur, S.; Deswal, G.; Chopra, B.; Dhingra, A.K.; Guarve, K.; Grewal, A.S. In silico docking based screening of constituents from Persian shallot as modulators of human glucokinase. *J. Diabetes Metab. Disord.* **2023**, *22*, 547-570, <https://doi.org/10.1007/s40200-022-01176-z>.
65. Sharma, P.; Thakur, A.; Goyal, A.; Singh Grewal, A. Molecular docking, 2D-QSAR and ADMET studies of 4-sulfonyl-2-pyridone heterocycle as a potential glucokinase activator. *Res. Chem.* **2023**, *6*, 101105, <https://doi.org/10.1016/j.rechem.2023.101105>.
66. Sharma, P.; Goyal, A.; Grewal, A.S. Design, synthesis and biological evaluation of novel sulfamoyl benzamides as allosteric activators of human glucokinase. *Chem. Biol. Lett.* **2024**, *11*(1), 657-657. <https://doi.org/10.62110/sciencein.cbl.2024.v11.657>.
67. Grewal, A.S.; Sharma, N.; Singh, S.; Arora, S. Molecular Docking Studies of Phenolic Compounds from *Syzygium cumini* with Multiple Targets of Type 2 Diabetes. *J. Pharm. Technol. Res. Manag.* **2018**, *6*, 125-133, <https://doi.org/10.15415/jptrm.2018.62009>.
68. Pires, D.E.V.; Kaminskas, L.M.; Ascher, D.B. Prediction and Optimization of Pharmacokinetic and Toxicity Properties of the Ligand. In *Computational Drug Discovery and Design*, Gore, M., Jagtap, U.B., Eds.; Springer New York: New York, NY, **2018**; pp. 271-284, https://doi.org/10.1007/978-1-4939-7756-7_14.
69. Pires, D.E.V.; Blundell, T.L.; Ascher, D.B. pkCSM: Predicting Small-Molecule Pharmacokinetic and Toxicity Properties Using Graph-Based Signatures. *J. Med. Chem.* **2015**, *58*, 4066-4072, <https://doi.org/10.1021/acs.jmedchem.5b00104>.

Publisher's Note & Disclaimer

The statements, opinions, and data presented in this publication are solely those of the individual author(s) and contributor(s) and do not necessarily reflect the views of the publisher and/or the editor(s). The publisher and/or the editor(s) disclaim any responsibility for the accuracy, completeness, or reliability of the content. Neither the publisher nor the editor(s) assume any legal liability for any errors, omissions, or consequences arising from the use of the information presented in this publication. Furthermore, the publisher and/or the editor(s) disclaim any liability for any injury, damage, or loss to persons or property that may result from the use of any ideas, methods, instructions, or products mentioned in the content. Readers are encouraged to independently verify any information before relying on it, and the publisher assumes no responsibility for any consequences arising from the use of materials contained in this publication.